Available online at www.sciencedirect.com
SCIENCE DIRECT®
NEUROCOMPUTING
ELSEVIER
Neurocomputing 58–60 (2004) 1203–1209
www.elsevier.com/locate/neucom

Simulation of neocortical epileptiform activity using parallel computing

Wim van Drongelen[a,*], Hyong C. Lee[a], Mark Hereld[b,c], David Jones[c], Matthew Cohoon[a], Frank Elsen[a], Michael E. Papka[b,c], Rick L. Stevens[b,c]

[a] *Department of Pediatrics, The University of Chicago, 5841 South Maryland Av MC 3055, Chicago 60637, USA*
[b] *Department of Computer Science, The University of Chicago, 5841 South Maryland Av MC 3055, Chicago, IL 60637-1470, USA*
[c] *Mathematics and Computer Science Division, Argonne National Laboratory, Argonne, IL 60439-4844, USA*

Abstract

A scalable network model intended for study of neocortical epileptiform activity was built on the pGENESIS neural simulator. The model included superficial and deep pyramidal cells plus four types of inhibitory neurons. An electroencephalogram (EEG) simulator was attached to the model to validate model behavior and to determine the contributions of inhibitory and excitatory neuronal populations to the EEG signal. We examined effects of overall excitation and inhibition on activity patterns in the network, and found that the network-bursting patterns occur within a narrow range of the excitation–inhibition space. Further, we evaluated synchronization effects produced by gap junctions during synchronous and asynchronous states.

Keywords: Epilepsy; Network bursting; Gap junction; Parallel computing; EEG

1. Introduction

The electroencephalogram (EEG) recorded from the scalp during epileptic seizures frequently shows abnormal bursting activity over large cortical areas. Because the EEG signal is a weighted sum of electrical currents originating from hundreds of thousands

* Corresponding author.
E-mail address: wvandron@peds.bsd.uchicago.edu (W. van Drongelen).

0925-2312/$ - see front matter © 2004 Elsevier B.V. All rights reserved.
doi:10.1016/j.neucom.2004.01.186

of cells, this type of measurement does not reveal much detail about the underlying activity. Experimental studies in animal models, and in slices from resected tissue from epilepsy patients, have demonstrated the nature of paroxysmal cellular behavior and network activity at a small scale (e.g. [2,6,17,18,22]). Modeling studies of bursting behavior have typically focused on intrinsic membrane properties, small neural networks, or larger networks with reduced complexity at the cellular level (e.g. [5,7,10,12,14,20]).

Our objective was to create a scalable network of neocortex ($1–10^5$ model neurons) with a high level of detail in both intrinsic properties and network function. This approach not only allows the study of underlying processes of pathological behavior in the brain, but can also provide a unique opportunity to understand the interrelationship of this type of behavior at different scales. The cells intrinsic properties and the network parameters of the model can be both examined for their role in evoking and sustaining seizure-like bursting. Our emphasis on neocortical circuitry is motivated by the fact that the epileptic foci in children are frequently found in neocortex. The results obtained with an earlier version of our model were reported previously [21].

2. Model

The neocortex is organized in six horizontal layers and shows vertical organization into modules, or (micro-)columns [15,16,19]. The canonical circuit for neocortex, first proposed by Douglas and Martin [9], was extended with additional inhibitory cell types for our model (Fig. 1). The major neural component of neocortex consists of two types of pyramidal cells: the *superficial neurons* in layers 2–3 (S_, Fig. 1) and *deep cells* in layers 5–6 (D_, Fig. 1). Similarly, inhibitory units in neocortex are commonly

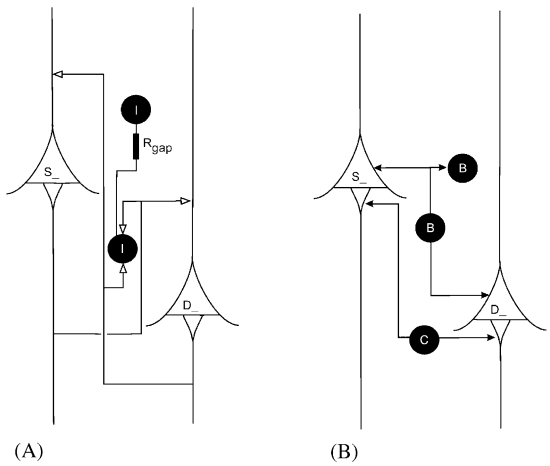

Fig. 1. Overview of cell types and connectivity. (A) Excitatory contacts including gap junctions depicted as a resistor between inhibitory cells (I); S_ and D_ symbolize the superficial and deep pyramidal cells. (B) Inhibitory synapses; inhibitory neurons are symbolized by B and C (basket and chandelier cells, respectively).

subdivided into different subtypes [9,16]. Basket cells (B, Fig. 1) inhibit the pyramidal cells soma, receive inputs from pyramidal cells, and connect with other interneurons [16,23]. Furthermore, Krimer and Goldman-Rakic [13] identified *3 types of basket cells*, which were classified on the basis of the range of the axon arbor. *Chandelier cells* (C, Fig. 1) also inhibit the initial segment of the pyramidal cell and receive inputs from the pyramidal cells [9,13]. Other types of inhibitory neurons were not included in the current model. Individual cells were modeled as multi-compartment units with Hodgkin and Huxley type Na^+ and K^+ channels [11], with the length and diameter of the cylindrical compartments adjusted to obtain similar intrinsic firing properties as the reduced and full models reported in [4].

In order to create a realistic cell density, the spacing between pyramidal cells was set to 5 μm. The spacing of the four types of inhibitory neurons was set to 3 times the spacing of the pyramidal cells. For a patch of 1×1 mm, the number of S_ and D_PYR cells is $2 \times 200 \times 200 = 80,000$ and for the four types of inhibitory cells equals $4 \times 66.6 \times 66.6 = 17,778$; this brings the ratio of pyramids/inhibitors to $\frac{4.5}{1}$ and the cell density to $\sim 10^5/\text{mm}^2$ of cortex. This cell density is in agreement with [6,8,15,16], where estimate ranged from 0.5×10^5 to $2 \times 10^5/\text{mm}^2$ with $\sim 80\%$ excitatory neurons. The average depth of the superficial pyramidal cells, the inhibitory neurons, and deep pyramidal cells was chosen to be 350, 900, and 1450 μm, respectively.

The excitatory and inhibitory connections in the micro-circuitry are depicted in Fig. 1. The pyramidal units (S_ and D_, Fig. 1A) have reciprocal excitatory circuitry. The inhibitory units (I, Fig. 1A) represent both basket and chandelier cell types (B and C, Fig. 1B). The connections were implemented with the *rvolumeconnect* command in pGENESIS [3]. This command allows one to specify which source cells connect to which target cells and at what connection probability. Associated commands, *rvolumeweight* and *rvolumedelay* determine the strength of the synaptic contacts and the conduction delays between source and destination cells. At a density of 10^5cells/mm^2 of neocortex, and assuming that every cell connects to every other, we would obtain $(10^5)^2 - 10^5 \approx 10^{10}$ contacts/mm^2. Taking the total number of synapses in the neocortex to be 3×10^{14} [16], and with a total cortical surface area estimated at 2.5×10^5 mm^2, results in $\sim 1 \times 10^9$ synapses/mm^2 of cortex. Given a potential of 10^{10} contacts, this translates into an overall connection probability of $\sim 10\%$. Consequently, this probability was used for the connection between pyramidal cells in the model.

According to Krimer and Goldman-Rakic [13], the probability of the connection from pyramidal units in layer 3 to basket cells is $\sim 25\%$ in 100 μm. We use this figure for all connections between pyramidal cells and all types of inhibitory neurons. A chandelier cell contacts 300 pyramidal cells in a 0.2–0.4 mm range [9]. Using the average (0.3 mm), containing 2×3600 pyramidal cells in our model, we obtain a probability $p = \frac{300}{7200} \approx 4\%$. Similarly, these authors estimate that each basket cell contacts 300 local pyramidal cells. Taking the wide arbor cells (WAC) with a dendritic span of 0.9 mm this equates to a probability of $300/(2 \times 32,400) \approx 0.5\%$. Similarly, the probability for medium arbor cells (MAC) with a 0.6 mm area is $300/(2 \times 14,400) \approx 1\%$, and for local arbor cells (LAC) with a 0.3 mm extent is $300/(2 \times 3600) \approx 4\%$.

Nieuwenhuys [16] describes large basket cells contacting up to 300 pyramidal cells and 50 other basket cells in their area (a ratio of $\frac{50}{300} \approx 17\%$). This ratio is in reasonable

agreement with [23] stating that 14% of small basket cell contacts are with interneurons. The 300 μm dendritic range of the LAC would be expected to contain $3\times20\times20=1200$ basket cells, which equates to a probability of $\frac{50}{1200} \approx 4\%$. The 600 μm arbors of MAC produces a probability of $50/(3\times40\times40) \approx 1.5\%$, and for the 900 μm span of WAC, $50/(3\times60\times60) \approx 0.7\%$.

Recent work shows that neocortical inhibitory neurons are often interconnected through gap junctions [1], and that the connections appear to occur between neighboring cells of the same type. Consequently, this feature was also implemented in the model (Fig. 1A) with a connection probability of 80%.

3. Results

The effects of strength of excitation (connections in Fig. 1A) and inhibition (connections in Fig. 1B) on spontaneous activity and bursting in a 1000-cell neural network are shown in Fig. 2. Each panel in Fig. 2 shows the superimposed activity of the S_PYR cell group during and after current is injected in one of the cells. This current injection (during the initial 50 ms) is necessary to start activity in the model. At low levels of excitation the model becomes quiet after stimulus offset, while high levels of

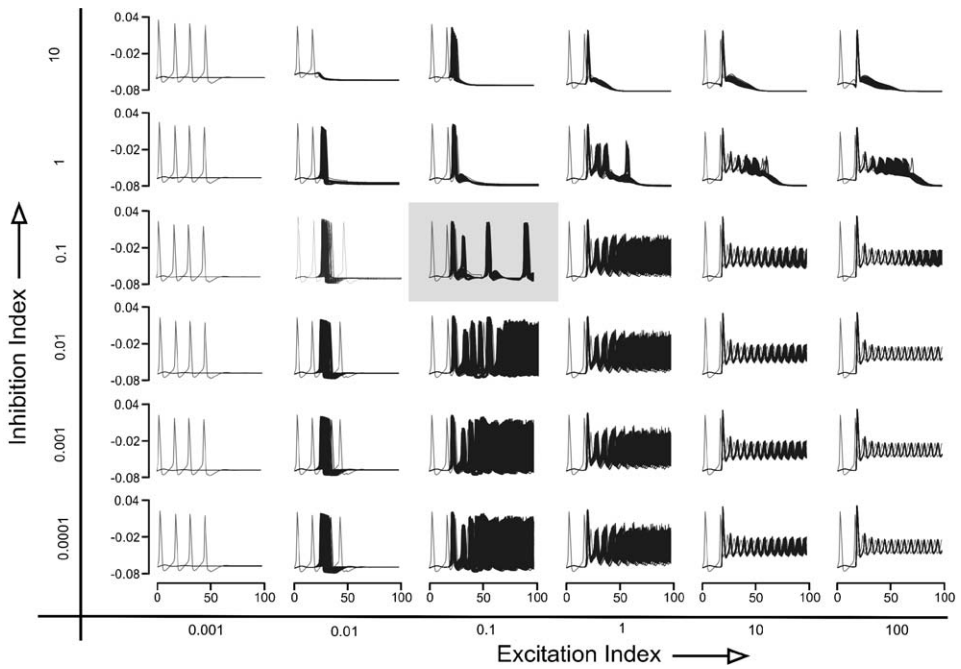

Fig. 2. Effect of overall levels of excitation and inhibition in a model with 1000 neurons. Details are explained in the text.

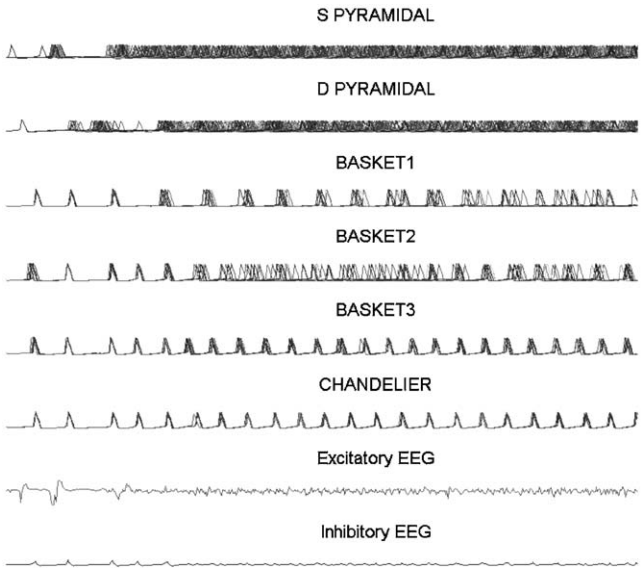

Fig. 3. A 300 ms epoch of activity in a small 160-cell network. Activities of both pyramidal cell types are superimposed in the two upper traces. The next four traces are superimposed activities of inhibitory cell types; note the relatively strong synchrony. The two lower traces are the contributions of the excitatory and inhibitory populations to the EEG signal. In this example $R_{gap} = 3 \times 10^8\ \Omega$.

excitation (> 10) produce severe signs of saturation in the cellular activities. In spite of the absence of intrinsic bursting properties in the model neurons, there is a clear area in this parameter space where the network continues to burst spontaneously after stimulus offset (gray rectangle, Fig. 2). The area around the bursting pattern in Fig. 2, is the most dynamic region in the excitation–inhibition space. In this area, the patterns can transition from inactivity to a bursty or continuous type of spontaneous activity. A similar area of network bursting was found at different sizes of the model (tested scales range between 0.64×10^3 and 10×10^3 cells).

Effects of the gap junctions between the inhibitory cells of the same cell type were evaluated by varying R_{gap} (Fig. 1A). During ongoing sustained activity, strong synchronization effects in the smallest cells (chandelier cells and small basket cells) can be observed at $R_{gap} = 3 \times 10^8\ \Omega$ (Fig. 3). The larger basket cells synchronize further at a level of $3 \times 10^7\ \Omega$. When all cell types in the model were in bursting mode (instead of tonically active), there was no observable difference between presence and absence of gap junctions.

The two lower traces in Fig. 3 show the contributions of the excitatory cells and the inhibitory populations to the field potential/EEG measured at the cortical surface. It can be seen that in spite of the asynchronous activity in the excitatory population and the relatively strong synchrony in the inhibitory cells, the contribution of the latter cell type to the EEG is relatively small.

4. Discussion

We have demonstrated that a model of neocortex with non-intrinsically bursting elements can generate a rich variety of activity patterns, including network bursting. It is significant that there seems to be a restricted space for network bursting that is accessible from different sides in the excitation–inhibition space (Fig. 2). Epilepsy is often considered as a hyper-excitatory state or a state with a lack of inhibition. Our data show that a hypothesis of an excitation–inhibition balance is too simple to explain a change of pattern into a bursting mode. Indeed in some instances, the model can be brought into the bursting mode by increasing excitation or by decreasing inhibition. However depending on the initial position in the excitation–inhibition space, other scenarios are clearly possible.

Our data also support the suggestion that the gap junctions may have a critical effect in synchronizing the inhibitory neuronal population [1] (Fig. 3). Without gap junctions, the synchrony in the inhibitory cell types, as shown in Fig. 3, is absent. However, the synchronizing effect is state dependent: i.e. during a network bursting mode as shown in Fig. 2, the effects of the gap junctions are not significant since the input to the inhibitory cells is already grouped in synchronized bursts. This finding indicates that gap junction dysfunction may play a role in the transition to a pathologic bursting state. However, during an ongoing seizure-like bursting state modulation of the resistance between the electrical couplings may not have an effect.

Acknowledgements

Supported by the Falk Grant and by the Mathematical, Information and Computer Sciences Division subprogram of the Office of Advanced Scientific Computing Research, US Department of Energy, Contract W-31-109-ENG-38.

References

[1] Y. Amitai, J.R. Gibson, M. Beierlein, S.L. Patrick, A.M. Ho, B.W. Connors, D. Golomb, The spatial dimensions of electrically coupled networks of interneurons in the neocortex, J. Neurosci. 22 (2002) 4142–4152.
[2] M. Avoli, A. Williamson, Functional and pharmacological properties of human neocortical neurons maintained in vitro, Prog. Neurobiol. 48 (1996) 519–554.
[3] J.M. Bower, D. Beeman, The Book of GENESIS, Springer, New York, 1998.
[4] P.C. Bush, T.J. Sejnowski, Reduced compartmental models of neocortical pyramidal cells, J. Neurosci. Methods 46 (1993) 159–166.
[5] E.T. Claverol, A.D. Brown, J.E. Chad, A large-scale simulation of the piriform cortex by a cell automaton-based network model, IEEE Trans. Biomed. Eng. 49 (2002) 921–935.
[6] B.W. Connors, Y. Amitai, Generation of epileptiform discharge by local circuits of Neocortex, in: P.A. Schwartzkroin (Ed.), Epilepsy, Cambridge University Press, New York, 1993, pp. 388–423.
[7] A. Destexhe, D. Pare, Impact of network activity on the integrative properties of neocortical pyramidal neurons in vivo, J. Neurophysiol. 81 (1999) 1531–1547.
[8] R. Douglas, C. Koch, M. Mahowald, K. Martin, The role of recurrent excitation in neocortical circuits, in: P.S. Ulinski, E.G. Jones, A. Peters (Eds.), Cerebral Cortex 13. Models of Cortical Circuits, Kluwer Academic/Plenum, New York, 1999, pp. 251–282.

[9] R.J. Douglas, K.A.C. Martin, Neocortex, in: G.M. Shepherd (Ed.), The Synaptic Organization of the Brain, Oxford University Press, Oxford, 1990, pp. 389–438.
[10] D. Golomb, Y. Amitai, Propagating neuronal discharges in neocortical slices: computational and experimental study, J. Neurophysiol. 78 (1997) 1199–1211.
[11] A.L. Hodgkin, A.F. Huxley, A quantitative description of membrane current and its application to conduction and excitation in nerve, J. Physiol. 117 (1952) 500–544.
[12] A. Kepecs, X.J. Wang, J. Lisman, Bursting neurons signal input slope, J. Neurosci. 22 (2002) 9053–9062.
[13] L.S. Krimer, P.S. Goldman-Rakic, Prefrontal microcircuits: membrane properties and excitatory input of local, medium and wide arbor interneurons, J. Neurosci. 21 (2001) 3788–3796.
[14] W.W. Lytton, T.J. Sejnowski, Simulations of cortical pyramidal neurons synchronized by inhibitory interneurons, J. Neurophysiol. 66 (1991) 1059–1079.
[15] V.B. Mountcastle, The columnar organization of the neocortex, Brain 120 (1997) 701–722.
[16] R. Nieuwenhuys, The neocortex. An overview of its evolutionary development, structural organization and synaptology, Anat. Embryol. 190 (1994) 307–337.
[17] M. Sanchez-Vives, D.A. McCormick, Cellular and network mechanisms of rhythmic recurrent activity in neocortex, Nat. Neurosci. 3 (2000) 1027–1034.
[18] M. Steriade, F. Amzica, D. Neckelmann, I. Timofeev, Spike-wave complexes and fast components of cortically generated seizures. II. Extra- and intracellular patterns, J. Neurophysiol. 80 (1998) 1456–1479.
[19] J. Szentagothai, The neuron network of the cerebral cortex: a functional interpretation, Proc. R. Soc. London B 201 (1978) 219–248.
[20] R.D. Traub, J.G. Jefferys, R. Miles, M.A. Whittington, K. Toth, A branching dendritic model of a rodent CA3 pyramidal neurone, J. Physiol. 481 (1994) 79–95.
[21] W. van Drongelen, M. Hereld, H.C. Lee, M.E. Papka, R.L. Stevens, Simulation of neocortical activity, Epilepsia 43 (Suppl. 7) (2002) 149.
[22] W. van Drongelen, H. Koch, C. Marcuccilli, F. Pena, J.-M Ramirez, Synchrony levels during evoked seizure-like bursts in mouse neocortical slices, J. Neurophysiol. 90 (2003) 1571–1580.
[23] Y. Wang, A.Gupta, M. Toledo-Rodriguez, C.Z. Wu, H. Markram, Anatomical, physiological, molecular and circuit properties of nest basket cells in the developing somatosensory cortex, Cerebral Cortex 12 (2002) 395–410.